MINIMIZING WHEEL SLIP IN RAILWAY LOCOMOTIVES WITH COUPLED PERMANENT MAGNET SYNCHRONOUS MOTORS

Shayak Bhattacharjee

Department of Physics,
Indian Institute of Technology Kanpur,
NH91, Kalyanpur,
Kanpur – 208016,
Uttar Pradesh, India

shayak@iitk.ac.in shayak12424@yahoo.in

Classification

PACS : 84.50.+d 05.45.Xt

Keywords : Back-emf triggered commutation, Coupled motors, Synchronized state, Wheel slip

Abstract

In this work I consider control strategies of permanent magnet synchronous motors in which the back-emf signal from the motor is used to achieve commutation of the six step driving circuit. I show that if the strategy is modified to connect multiple motors in a cyclic chain, then a collective synchronized state is favoured. The stability of this state can be exploited in the bogies of a railway locomotive to automatically terminate wheel slipping episodes.

* * * * *

Introduction

Permanent magnet synchronous motors (PMSMs) are the motor of choice for high performance applications such as electric traction [1,2]. Their primary advantage over induction motors arises from their high magnetic field strength, which enables powerful motors to be employed at a low unsprung mass per axle. Typically, a power density exceeding 1 kW/kg can be extracted from these motors while their asynchronous counterparts are limited to 0.7 kW/kg or lower [3]. Further, the flux weakening characteristics of PMSMs are better than those of induction motors, which are limited by their voltage curve. This translates to a higher power output over a larger range of speed. Despite these manifest plus points PMSMs are presently limited to a handful of locomotives and trainsets, all in the extremely high end category, such as the AGV mentioned in [3]. One of the reasons behind this is that effective control of PMSMs is greatly more difficult than that of induction motors. The two primary control mechanisms are field oriented control (FOC) [4,5] and direct torque control (DTC) [6-10]. Both of these require accurate determination of the rotor's position (which is complicated) and involve lengthy calculations in the field weakening regime [11,12].

A class of control strategy which bypasses these complications is the one where a six step drive circuit is used and the commutation is sequential, being triggered by the back-emf of the motor. This strategy is common in brushless dc motor drives [13,14] as it is robust and cheap. It also found an application in the BB 26000 locomotive developed by Alstom [15]. In the next generation of Alstom locomotive however, induction motor was given preference to PMSM, primarily because the drive strategies gave greater control over the motor's dynamics. Indeed, one of the problems from which BB 26000 suffered was that of continuous wheel slipping with heavy load in drizzling weather. In this paper I show that a simple variation on the basic strategy – namely, triggering the commutation of one motor by the back-emf from *another* motor – can eliminate this problem entirely. In the course of this derivation, I obtain certain closed form solutions of the highly nonlinear PMSM dynamical equations, which are hard to come by in the literature (some explicit solutions of the induction motor equations have been presented by Takahashi, Isao and Noguchi, Toshihiko [6]).

1. Description and dynamic modeling

Figure 1 shows the schematic representation of the conventional setup (Fig. 1A) as well as the proposed modification (Fig. 1B). The simplest possible system, i.e. two coupled motors, has been chosen in the latter case. The inverters may be voltage source or current source. The latter is used in BB 26000 but in this paper I will work with a voltage source as that provides automatic flux weakening. The space phasor notation has been used, and the voltmeter V attached to each motor measures its induced emf vector. The sequential commutation is implemented by stipulating that the inverter output voltage is $-A\exp(j\varphi)$ times the induced voltage. Of course, this assumes continuity of the output voltage vector; to model the six step waveform, the angle of the vector must be rounded off to the nearest multiple of 60^{o}. The discretization affects only the higher harmonics and not the fundamental harmonic, which is of interest in this paper. The cyclic connection scheme can easily be extended to the cases of three, four or more motors.

The first step in any control application is to understand the dynamics of the system which is being controlled. Various approaches exist for modelling the dynamics of permanent magnet motors, for example the *d-q* model [16,17] which can account for both surface mounted as well as interior mounted motors. The synchronization phenomenon which I will show in this paper is very general however and cannot depend on the specific constructional details of the motors being used. Hence I will use the simplest possible PMSM model, which assumes that there is no pole saliency and that the magnetic fields can be written in terms of surface currents (i.e. currents per unit circumferential length) flowing in the rotor. As it turns out, the analysis using even this most simplified model is quite difficult and complications in the model only serve to remove the analytic solutions beyond reach.

The voltage-current dynamics of a general cylindrical motor structure with sinusoidal current distributions has been obtained in [18,19] and I quote the relevant equation below, where I have assumed the polarity of the motor to be 2 without loss of generality :

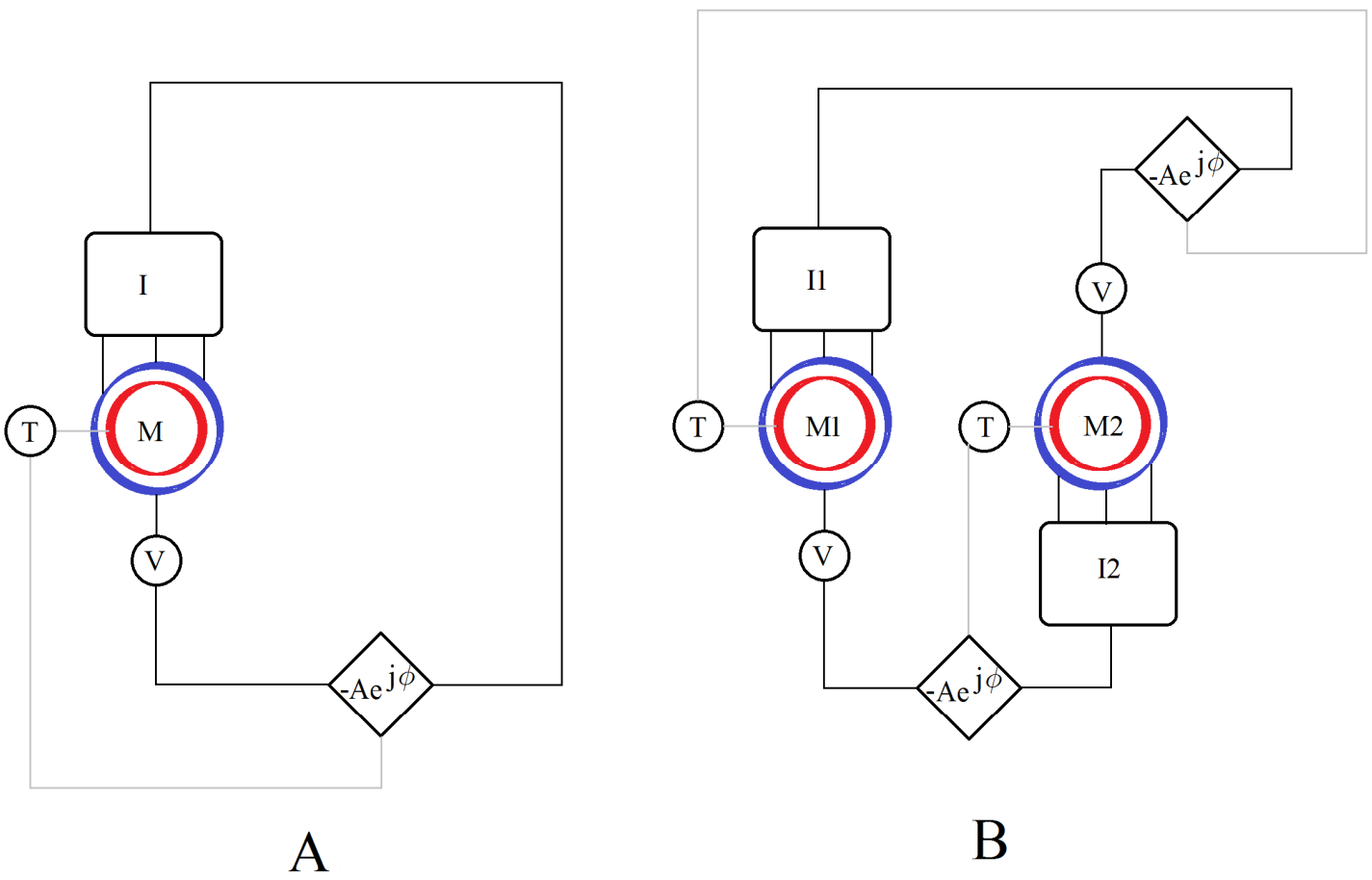

Figure 1 : *(A) shows the schematic diagram of the single motor controlled using sequential commutation triggered by the back-emf. I is the inverter and M the traction motor. The voltmeter V measures the back-emf vector which is multiplied by the complex number –Aexp(jφ) to obtain the voltage vector desired from the inverter. T denotes the torque observer whose function is to measure the torque of the motor and adjust φ accordingly. The connections of the torque observers have been shown in light grey to create a contrast with the main feedback loop (black). (B) shows the arrangement of two coupled motors where the back-emf of one motor forces the commutation of the other motor.*

$$\begin{bmatrix} 1+\tau_r\left(\frac{\mathrm{d}}{\mathrm{d}t}-\mathrm{j}\omega\right) & \delta_1\tau_r\left(\frac{\mathrm{d}}{\mathrm{d}t}-\mathrm{j}\omega\right) \\ \delta_2\tau_s\frac{\mathrm{d}}{\mathrm{d}t} & 1+\tau_s\frac{\mathrm{d}}{\mathrm{d}t} \end{bmatrix}\begin{bmatrix}\mathbf{K}_r\\ \mathbf{K}_s\end{bmatrix}=\begin{bmatrix}0\\ \mathbf{V}\end{bmatrix} \quad . \tag{1}$$

Here, $\mathbf{K}_r$ and $\mathbf{K}_s$ are the rotor and stator surface current phasors formed by adding the coefficient of the cosθ component and j times the coefficient of the sinθ component of the corresponding spatial distribution. Likewise $\mathbf{V}$ is the applied voltage phasor normalized to a surface current by multiplication of some appropriate constant factor. τ_r and τ_s are the time constants of the rotor and stator and δ_1 and δ_2 are numerical constants lying between 0 and 1 and depending on the motor geometry.

Now for a permanent magnet rotor the magnetic field strength is fixed hence the magnitude of the vector $\mathbf{K}_r$ is also fixed. Since the magnetization is uniform relative to the rotor, in the stator frame it changes direction as the rotor rotates. The angle made by $\mathbf{K}_r$ is dependent on the angle θ_r made by the rotor with some fixed reference line in the stator frame, hence I can write

$$\mathbf{K}_r = K_0\exp(\mathrm{j}\theta_r) \quad , \tag{2/1}$$

$$\dot{\mathbf{K}}_r = \mathrm{j}K_0\dot{\theta}_r\exp(\mathrm{j}\theta_r) \quad , \tag{2/2}$$

where K_0 is a constant and overhead dots indicate the time derivative. For the permanent magnet rotor, there is no current dynamics and no time constant hence the first row of (1) is irrelevant. For reasons which will be

explained later, I assume that there are no amortisseur windings on the rotor. Substituting (2) into (1) I get the voltage-current equation for the PMSM as

$$\tau_s \dot{\mathbf{K}}_s + \mathbf{K}_s = \mathbf{V} - \mathrm{j}\delta_2 \tau_s K_0 \dot{\theta}_r \exp(\mathrm{j}\theta_r) \quad . \tag{3}$$

The second term on the right hand side (RHS) of this equation is in fact the back-emf which is measured in the control strategies considered here.

To complete the system I must write Newton's law for the motor. The angular velocity is defined as

$$\omega = \dot{\theta}_r \quad , \tag{4}$$

and its dynamics follows the same equation as does the induction motor :

$$J\dot{\omega} = C\mathbf{K}_r \cdot (-\mathrm{j}\mathbf{K}_s) - \Gamma \quad , \tag{5}$$

in which J is the moment of inertia of the motor and load, C is a positive constant depending on the motor properties and Γ is the drag torque.

Substituting the sequential commutation condition in (3) to (5), the dynamic model of the single motor system in Fig. 1A can be written as

$$\dot{\mathbf{K}}_s + \frac{\mathbf{K}_s}{\tau_s} = \mathrm{j}\delta_2 K_0 \left(A\mathrm{e}^{\mathrm{j}\varphi} - 1 \right) \dot{\theta}_r \exp(\mathrm{j}\theta_r) \quad , \tag{6/1}$$

$$J\ddot{\theta}_r = C\mathbf{K}_r \cdot (-\mathrm{j}\mathbf{K}_s) - \Gamma \quad . \tag{6/2}$$

For the two-motor system of Fig. 1B, which is the primary focus of this paper, I can reasonably assume that the internal motor parameters such as K_0, τ_s, δ_2 and C are identical for both motors. However, J and Γ need not be so and, with obvious labels on quantities like $\mathbf{K}_s$ for the two motors, the system equation reads as :

$$\dot{\mathbf{K}}_{s1} + \frac{\mathbf{K}_{s1}}{\tau_s} = \mathrm{j}\delta_2 K_0 \left[-\dot{\theta}_{r1} \exp(\mathrm{j}\theta_{r1}) + A\mathrm{e}^{\mathrm{j}\varphi} \dot{\theta}_{r2} \exp(\mathrm{j}\theta_{r2}) \right] \quad , \tag{7/1}$$

$$\dot{\mathbf{K}}_{s2} + \frac{\mathbf{K}_{s2}}{\tau_s} = \mathrm{j}\delta_2 K_0 \left[-\dot{\theta}_{r2} \exp(\mathrm{j}\theta_{r2}) + A\mathrm{e}^{\mathrm{j}\varphi} \dot{\theta}_{r1} \exp(\mathrm{j}\theta_{r1}) \right] \quad , \tag{7/2}$$

$$J_1\ddot{\theta}_{r1} = C\mathbf{K}_{r1} \cdot (-\mathrm{j}\mathbf{K}_{s1}) - \Gamma_1 \quad , \tag{7/3}$$

$$J_2\ddot{\theta}_{r2} = C\mathbf{K}_{r2} \cdot (-\mathrm{j}\mathbf{K}_{s2}) - \Gamma_2 \quad . \tag{7/4}$$

By writing the d-q forms of these equations it is easy to verify that (6) is fourth order nonlinear while (7) is eighth order nonlinear. To prove the curbing of wheel slip in the coupled system (7), I will need to solve it explicitly. At this point it should be clear why a more difficult motor model would have rendered the system completely intractable. Before concluding this Section I mention the parameter values which will be used in simulations. I make the numerical values of various quantities close to what they might actually be in SI units for a typical traction motor. I take K_r and K_0 in Amperes with the relevant multiplication factors implicit, and summarize the values in Table 1.

φ =	0.5236 (30°)	τ_s =	1	δ_2 =	1/2	K_0 =	200
A =	3	C =	1/6	J =	2000	Γ =	2000 to 5000

Table 1 : *Parameter values used for simulation purposes.*

It should also be noted that all simulations are based on the d-q representations of (6) or (7) and not on any intermediate or approximate dynamical equations.

2. Solving the motor dynamics

In this Section I will solve the coupled equations (7) to demonstrate the automatic curbing of wheel slip. Prior to taking on (7) however, I will have a look at the single motor system (6).

A. *Prelude : the single motor system*

There are two reasons why it is worthwhile to spend some time with (6) before going on to (7). Firstly, the single motor analysis provides physical insight which will prove invaluable for overcoming the technical challenges posed by (7). Secondly and more importantly, when the wheels of the locomotive are rolling without slipping, then all the traction motors are by definition in a collectively synchronized state whose dynamics is governed by (6). To elaborate on this, the rolling without slipping condition means that at any instant, the angular velocity of each axle (and hence each motor) is equal to the train's linear velocity divided by the wheel radius. If the initial angles made by the rotors are equal (and they can always be assumed as such by suitably adjusting φ for each motor) then the positions and velocities of all the rotors at any instant become equal. This immediately forces the equality of all the induced emfs and hence of the applied voltages and currents and output torques. Even if the various output torques somehow become different during operation (say there is an error by the controller of one motor) then too the rolling without slipping condition will force the equality of the angular velocities, with the torque heterogeneities being compensated by ground friction. The purpose of the torque observers is precisely to sense such heterogeneity and smoothen it by adjusting φ for the concerned motors. When this step is done, all the motors will again behave identically. Clearly, in this mode of operation, the dynamics of one motor i.e. the system (6) will be sufficient to describe that of the whole lot.

I start the analysis by considering the steady state solutions of (6). The archetypal steady state of a motor corresponds to rotation at a constant rate ω^* : in this case, $\theta_r=\omega^* t$ and K_s acquires a form (...)exp(j$\omega^* t$). Since the time constant for a traction motor (say 1 s) is typically much greater than its rate of rotation (say 1000 rpm or 100 rad/s), the effect of the second term of the left hand side (LHS) of (6a) is generally negligible. This amounts to the statement that the stator becomes resistanceless. In this limit, the steady state stator current becomes

$$\mathbf{K}_s^s = \delta_2\left(A\mathrm{e}^{\mathrm{j}\varphi}-1\right)K_0\,\mathrm{e}^{\mathrm{j}\omega^* t} \quad , \tag{8}$$

where the superscript s denotes steady state. This current vector can be resolved into two components – the induced current and the applied current; since the stator is linear (an R-L circuit) these two are simply added. The former is located directly opposite the rotor and contributes nothing to the motor torque. The latter is located an angle φ ahead of the rotor current phasor, and if its magnitude be denoted by k_s (small k here), the torque on the rotor can be written as $CK_0k_s\sin\varphi$. This shows that φ is in fact the torque angle.

Since the induced voltage is proportional to the rotation speed, so is the applied voltage and (6) describes a Volts/Hz strategy. After a certain speed however, this strategy will no longer be feasible as the inverter will reach its rated output. Beyond this point the best I can do is to supply the rated voltage while maintaining φ at the maximum torque value of 90^o. Hence A will now acquire the form B/ω and (8) implies that the applied current will start weakening as $1/\omega$ while the induced current will remain constant in magnitude. This of course is the flux weakening regime. Like the applied current, the torque will vary as $1/\omega$ which implies that the power will become constant. Since there is no upper limit to the speed at which I can provide constant voltage at the desired phase, it follows that constant power operation is possible over a very wide range of speed.

The presence of j in (6) makes its analysis complex hence I write

$$\mathbf{K}_s = K_s\exp\left(\mathrm{j}\theta_s\right) \quad . \tag{9}$$

Since the magnitude of the stator current phasor can vary (unlike that of the rotor current phasor), its derivative evaluates to

$$\dot{\mathbf{K}}_s = \left(\dot{K}_s + \mathrm{j}K_s\dot{\theta}_s\right)\exp\left(\mathrm{j}\theta_s\right) \quad , \tag{10}$$

and in terms of θ_r and θ_s (6b) can be written as

$$J\ddot{\theta}_r = CK_0K_s\sin(\theta_s-\theta_r)-\Gamma \quad . \tag{11}$$

I now go back to the steady state solution (8) to start the dynamic analysis of (6). The linearity of the stator means that its current can always be expressed as a sum of steady state (i.e. particular) and transient (i.e. homogeneous) solutions. If there is a difference between the particular solution and the actual current at any time, then that difference constitutes the transient stator current. Now, at high rotor speeds where the resistanceless assumption (i.e. $\tau_s \rightarrow \infty$) is valid, the magnitude of the steady state stator current phasor, as well as the angle it makes with the rotor, are independent of the speed. Hence if steady state is attained once and after that if there is a finite change in rotor speed without an abrupt change in its position (the latter being physically implausible anyway) then the particular solution before the change, which equals the actual current before the change, is exactly equal to the particular solution after the change. This implies that *there is no transient current generated by a change in rotor speed, and that the torque angle* φ *between the applied stator current and the rotor current remains constant throughout as the motor speed goes up and down*. A corollary of this argument is that a change in load, which causes changes in acceleration and speed, does not generate transients.

I now verify this claim mathematically by linearizing the system (with resistanceless stator) about its normal (steady state) operating point, which I assume is characterized by the variables K_s^*, $\theta_s^*=\omega^* t+\theta^*$, $\theta_r^*=\omega^* t$. Note that φ does not equal θ_s-θ_r ! I let ΔK_s, $\Delta\theta_s$, $\Delta\theta_r$ and $\Delta\omega$ be the departures of these four variables from their steady state values. Using the definitions of A, φ and θ^* and the steady state equation (8), I obtain the relations $A\sin(\varphi-\theta^*)+\sin\theta^*=0$ and $\delta_2 K_0\left[A\cos(\varphi-\theta^*)-\cos\theta^*\right]=K_s{}^*$, which yield the dynamic matrix :

$$\begin{bmatrix} \Delta\dot{K}_s \\ \Delta\dot{\theta}_s \\ \Delta\dot{\theta}_r \\ \Delta\dot{\omega} \end{bmatrix} = \begin{bmatrix} 0 & \delta_2 AK_0K_s{}^*\omega^* & -\delta_2 AK_0K_s{}^*\omega^* & 0 \\ -\dfrac{\omega^*}{K_s{}^*} & 0 & 0 & 1 \\ 0 & 0 & 0 & 1 \\ -CK_0\sin\theta^* & \dfrac{C}{J}K_0K_s{}^*\cos\theta^* & -\dfrac{C}{J}K_0K_s{}^*\cos\theta^* & 0 \end{bmatrix} \begin{bmatrix} \Delta K_s \\ \Delta\theta_s \\ \Delta\theta_r \\ \Delta\omega \end{bmatrix} \quad . \tag{12}$$

The consequence of the structure (12) is that if there is no abrupt change in the magnitude of K_s or in the position of the stator or rotor current phasors, then a perturbation in rotor speed neither grows nor decays in time. Further, the stator current phasor remains unchanged in magnitude and both the stator and rotor current vectors make a seamless transition to rotation at the new speed $\omega^*+\Delta\omega$. This verifies what I concluded on the basis of the argument i.e. the change in speed is transientless and preserves the torque angle. It also reveals at once the fatal weakness of the drive circuit of Fig. 1A – if a wheel somehow starts to slip and accelerate out of hand, the controller will do nothing about it.

The ground has now been prepared for a discussion of the solutions of the coupled system (7). As a final comment, let me examine the range of validity of the resistanceless limit upon which the entire argument is based. The limit is bonafide if $\tau_s >> 1/\omega$. For a traction motor with $\tau_s \approx 1$ s, $\omega \approx 20$ rad/s or 200 rpm is good enough for the approximation to hold. For a typical loco, this corresponds to a speed of 10-12 km/hr, which is really small. Thus the argument is bona fide over nearly the entire range of the loco speed (which generally goes up to 150 km/hr or more).

B. *Actual solution : the coupled system*

Wheel slip on any axle occurs when the frictional coefficient between the corresponding wheel and rail is low and the axle's motion becomes independent of that of the train. The high values of J and Γ typical of a traction motor all arise from the enormous mass of the train as a whole; when one axle disengages from the train, its effective J and Γ reduce drastically. Further, the dynamics of the slipping axle must be evaluated in a standalone manner, uncoupled from the dynamics of the whole train. To mathematically model the scenario I assume that motors 1 and 2 were running in steady state of the perfectly synchronized state when axle 2 suddenly started to slip,

sharply reducing J and Γ for motor 2. Since motor 1 does not slip, its J and Γ remain high. For simulation purposes, ω^* is taken as 100, Γ_1 is set just above 5000, J_1 treated as 2000, J_2 assigned the value 2 and Γ_2 assumed to be equal to zero.

Analysis of the system (7) starts from the fact that the transition from collective mode to wheel slip is a change in load which, under the ambit of the resistanceless condition, generates no transients. Thus the only stator currents to worry about are the applied currents (induced currents give zero torque as before). Since the two stators are identical, the magnitudes of the applied currents on both motors are equal and constant. The constant torque angle ($=\varphi$) condition is re-interpreted as constancy of the angle (at the value φ) between the applied stator current phasor of one motor and the rotor current phasor of the other. Finally, since the torque on each motor varies as the sine of its own torque angle (the angle between its own rotor and applied stator current phasors), I get the reduced system of equations as

$$J_1\ddot{\theta}_{r1} = CK_0k_s\sin\left(\varphi+\theta_{r2}-\theta_{r1}\right)-\Gamma_1 \quad , \tag{13/1}$$

$$J_2\ddot{\theta}_{r2} = CK_0k_s\sin\left(\varphi+\theta_{r1}-\theta_{r2}\right)-\Gamma_2 \quad . \tag{13/2}$$

Thus the order of the system has been reduced from eight to four, but the equations are still heavily nonlinear. Since the initial conditions featured uniform rotation at speed ω^*, I define the deviations $\varepsilon_1=\theta_{r1}-\omega^*t$, $\varepsilon_2=\theta_{r2}-\omega^*t$ and write (13) in terms of $\varepsilon_{1,2}$ as

$$J_1\ddot{\varepsilon}_1 = CK_0k_s\sin\left(\varphi+\varepsilon_2-\varepsilon_1\right)-\Gamma_1 \quad , \tag{14/1}$$

$$J_2\ddot{\varepsilon}_2 = CK_0k_s\sin\left(\varphi+\varepsilon_1-\varepsilon_2\right) \quad , \tag{14/2}$$

in the latter of which I have made the substitution $\Gamma_2=0$ as that causes a slight reduction in the bookkeeping work. The key realization now is that because of the large disparity in the sizes of J_1 and J_2, there will also be a large disparity in the time scales at which ε_1 and ε_2 will work. In particular, ε_1 will vary slowly as motor 1 is burdened by the weight of the whole train while ε_2 will vary quickly as the light-hearted motor 2 can jump about at will. Further, since ε_1 starts from the value 0 (so does ε_2 by dint of the initial conditions), its small rate of variation implies that it itself will remain small at short times after the initiation of slip. These descriptions suggest that the system (14) may be amenable to a perturbative treatment combining the Lindstedt Poincare and separation of scales [20] techniques.

The first step is to write ε_2 as a series using ε_1 as the expansion parameter :

$$J_2\left(\ddot{\varepsilon}_{20}+\varepsilon_1\ddot{\varepsilon}_{21}+.....\right) = CK_0k_s\left[\sin\left(\varphi-\varepsilon_{20}\right)-\varepsilon_1\left\{\cos\left(\varphi-\varepsilon_{20}\right)-\cos\left(\varphi-\varepsilon_{20}\right)\varepsilon_{21}\right\}+.....\right] \quad , \tag{15}$$

in which ε_1 is assumed constant on account of its slow variation. Equating powers of ε_1 in (15), the zeroth order equation emerges as

$$J_2\ddot{\varepsilon}_{20} = CK_0k_s\sin\left(\varphi-\varepsilon_{20}\right) \quad . \tag{16}$$

The initial conditions are that ε_{20} and its derivative are both zero at $t=0$. Equation (16) is the well known equation for a pendulum – its solutions are oscillatory with frequency ν which equals $\left(CK_0k_s/J_2\right)^{1/2}$ for small oscillation amplitude (which is possible if φ is small) and acquires a correction as the oscillation amplitude increases. Thus I immediately obtain that, to largest order, the slipping axle shows oscillatory i.e. bounded motions.

And what happens to the loaded motor ? To find that out I must plug in the solution for ε_2 into (14/1). Specifically, the largest order solution for ε_1 will follow from substitution of the largest order ε_2 i.e. ε_{20} into (14/1); for this purpose I solve (16) to get

$$\varepsilon_{20} = \varphi\left(1-\cos\nu t\right) \quad . \tag{17}$$

Since v denotes a fast time scale, (17) will get averaged while solving for ε_1 and the specific value of v is not relevant. Note however that (17) satisfies the initial conditions for (16) – this is important despite the averaging. Substituting (17) into (14/1) and using the smallness of ε_1 I get

$$J_1\ddot{\varepsilon}_1 = CK_0k_s\left[\sin\left(2\varphi-\varphi\cos\nu t\right)-\varepsilon_1\cos\left(2\varphi-\varphi\cos\nu t\right)\right]-\Gamma_1 \quad . \tag{18}$$

At this point, any tendency to naively average $\cos\nu t$ and $\sin\nu t$ terms to zero must be curbed; since they occur as arguments of trigonometric functions, it is the outer functions which have to be averaged over. For this I first separate the ac and dc parts of their arguments using the formulae for sines and cosines of sums; I then use the identities

$$\frac{1}{2\pi}\int_0^{2\pi}\sin\left(x\cos\beta\right)\mathrm{d}\beta = 0 \quad , \tag{19/1}$$

$$\frac{1}{2\pi}\int_0^{2\pi}\cos\left(x\cos\beta\right)\mathrm{d}\beta = \mathrm{J}_0\left(x\right) \quad , \tag{19/2}$$

where $\mathrm{J}_0(x)$ denotes the Bessel function of the first kind (no italics on 'J'). Using these (18) can be averaged over the fast scale to get

$$J_1\ddot{\varepsilon}_1+\left[CK_0k_s\cos\left(2\varphi\right)\mathrm{J}_0\left(\varphi\right)\right]\varepsilon_1 = CK_0k_s\sin\left(2\varphi\right)\mathrm{J}_0\left(\varphi\right)-\Gamma_1 \quad . \tag{20}$$

Note that (20) can have two types of solutions – trigonometric functions for $\varphi<45^{\circ}$ and hyperbolic functions for $\varphi>45^{\circ}$. Since the simulation motor features the former case, I treat that one in detail, observing that the procedure remains identical for the other case. The formal solution of (20) is the particular integral (a constant) added to the homogeneous solutions which take the form

$$\varepsilon_1^{(h)} = P\cos\Omega t+Q\sin\Omega t \quad \text{, where} \tag{21/1}$$

$$\Omega^2 = \frac{CK_0k_s\cos\left(2\varphi\right)\mathrm{J}_0\left(\varphi\right)}{J_1} \quad . \tag{21/2}$$

The boundary conditions (ε_1 and its derivative at t=0 are zero) yield the complete formal solution of (20) as

$$\varepsilon_1 = \frac{CK_0k_s\sin\left(2\varphi\right)\mathrm{J}_0\left(\varphi\right)-\Gamma_1}{\Omega^2}\left(1-\cos\Omega t\right) \quad . \tag{22}$$

Thus, an approximate formal solution for ε_1 has been obtained. I keep repeating the word 'formal' because from a physical viewpoint the solution (22) is junk : the value of the particular solution and the amplitude of the oscillations could be anything depending on the motor parameters – maybe 1, maybe 1000 – and (22) does not in any way recognize that ε_1 is periodic with period 2π. The absurdity of this solution is even more apparent when $\varphi>45^{\circ}$ and the homogeneous solutions are hyperbolic. The problem occurs because (20) was derived assuming ε_1 to be small, so I cannot expect its solution to hold good when ε_1 is not small. The thing to hope for is that the formal solution matches the physical solution when t is small (compared to $1/\Omega$) because in this limit the formal solution too is small. For small t, I expand the cosine in (22) to leading order in t and use that $CK_0k_s\sin\varphi=\Gamma_1$ to obtain

$$\varepsilon_1 = \frac{\left(2\cos\varphi\cdot\mathrm{J}_0\left(\varphi\right)-1\right)\Gamma_1}{2J_1}t^2 \quad . \tag{23}$$

Before proceeding further let me compare this analytic solution with the exact (simulation) solution upto a time of 1 unit, which is intermediate between the slow and fast time scales : (23) is delightfully accurate (Fig. 2).

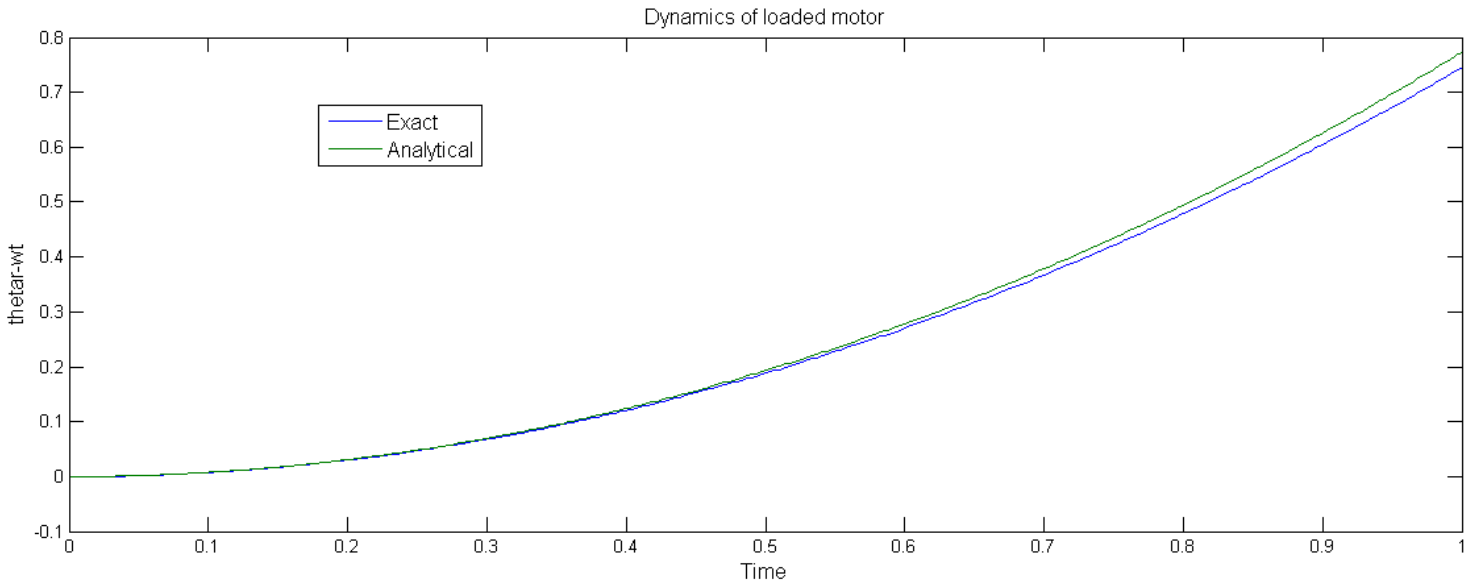

Figure 2 : [*Simulation results] The case of one slipping axle, which has been discussed extensively in the text, is simulated. The blue curve shows* ε_1 *from the simulation as a function of time while the green curve shows the analytic result, (23).*

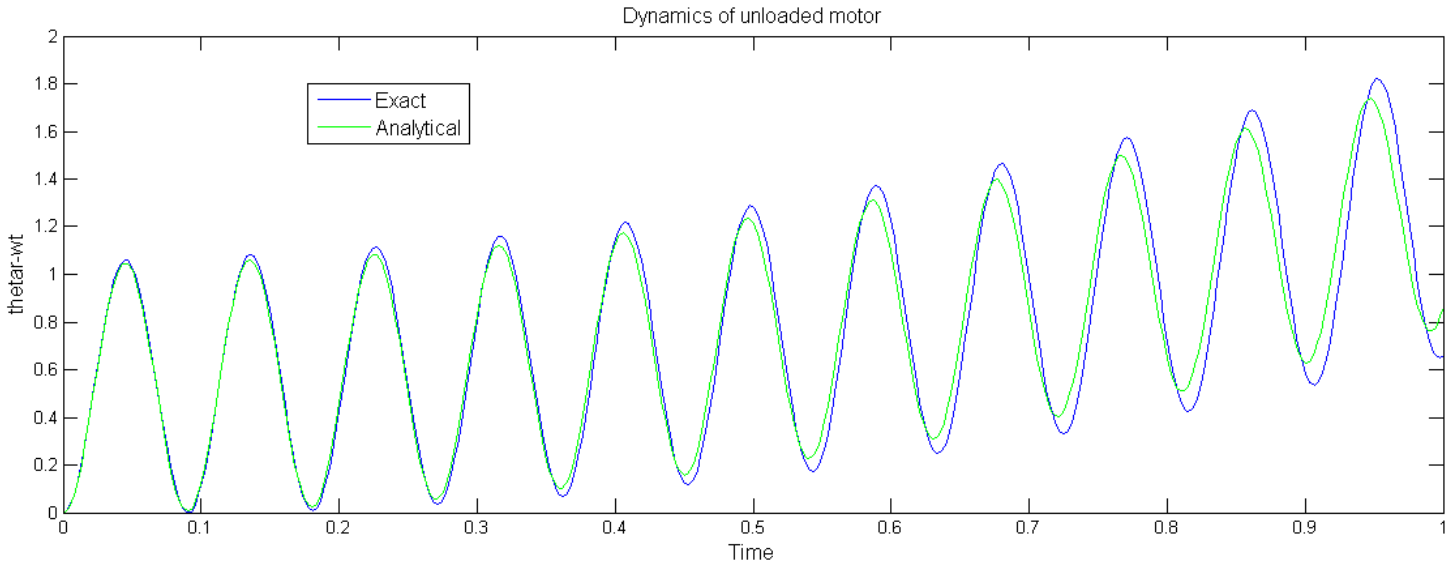

Figure 3 : *[Simulation results] The time trace of* ε_2 *from the simulation (blue) is compared with the analytical prediction (green). For greater accuracy, the analytic curve has been obtained by numerically integrating the (analytically derived) pendulum equation (16) and adding the result to the calculated* ε_1 *from (23).*

Encouraged by the success of this analytical prediction, let me return to the unloaded motor. Balancing terms of order ε_1 in (15), I can see that one solution which immediately satisfies the resulting equation is $\varepsilon_{21}=1$. Since this solution also satisfies the boundary conditions associated with the system, I conclude that it is the only solution. Physically it means that the unloaded rotor is oscillating about the instantaneous position of its stator current, whose variation can be considered adiabatic. The position of this current is just $\varepsilon_1+\varphi$ hence the centre of the rotor's oscillations must also be $\varepsilon_1+\varphi$. Thus I get the solution function

$$\varepsilon_2 = \varphi\left(1-\cos\nu t\right)+\varepsilon_1 \quad . \tag{24}$$

Indeed, this prediction too is borne out by the simulation, Fig. 3.

Now the assumption of Γ_2=0 in (14/2) is idealized. In reality, the slipping axle is subjected to small but nonzero frictional forces which try to oppose the relative motion between wheel and rail. At a basic level I may model the friction as a damping term proportional to $\dot{\varepsilon}_2$ through a constant γ. When such a term is inserted into (16), the oscillations decay in time and (24) acquires the form

$$\varepsilon_2 = \varepsilon_1 + \varphi\left[1 - \alpha e^{-\gamma t}\cos\left(\nu t + \beta\right)\right] \quad , \tag{25}$$

where the parameters α and β are required to satisfy the boundary conditions of the modified (16). Note that the specific form (23) for ε_1 ceases to hold when the damping is inserted but that does not affect the validity of (25). Clearly, for t larger than $1/\gamma$, the solution (25) tends to

$$\varepsilon_2 = \varepsilon_1 + \varphi \quad , \tag{26}$$

implying that the two motors again get synchronized, making a relative angle of φ between their rotors. This completes the proof of stability of the synchronized state.

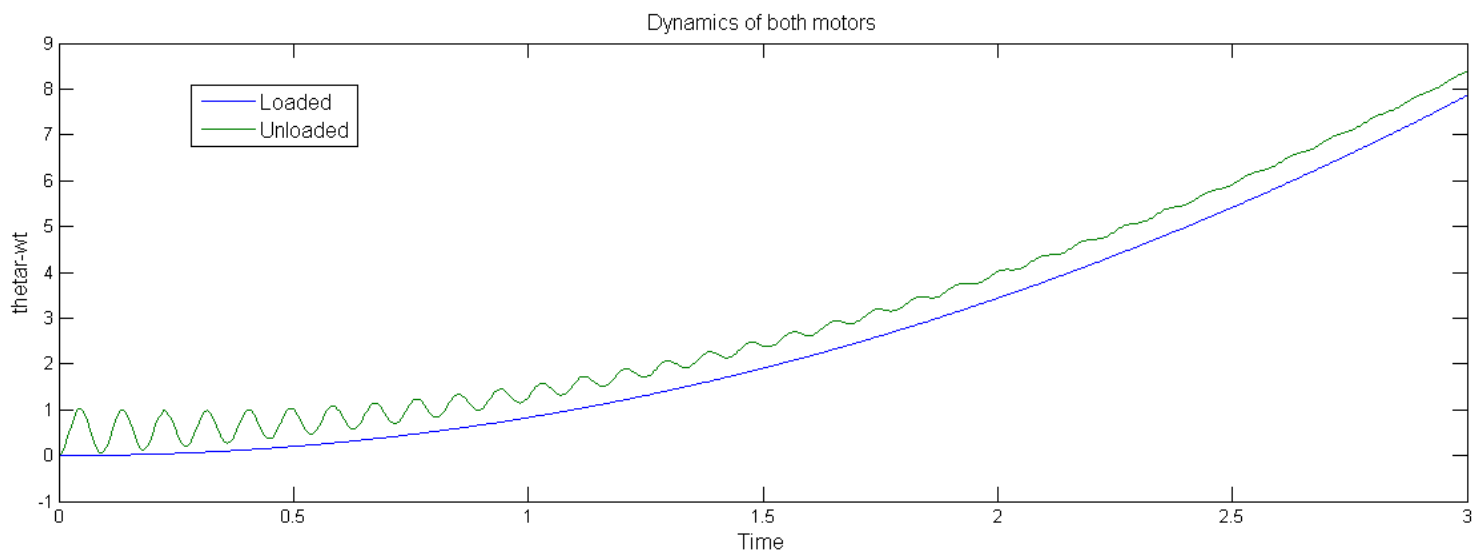

Figure 4 : *[Simulation results] Time traces of ε_1 (blue) and ε_2 (green) with a velocity-proportional damping term incorporated into the dynamic equation of the latter. The eventual outcome is clearly a re-synchronization of the two motors.*

The truth behind (25) and (26) is brought out by simulations (Fig. 4), where a damping term with time constant 1/5 has been tacked on to the dynamic equation of the unloaded motor. It confirms that *after a transient wheel slip episode, the system automatically returns to synchronism with no intervention on the part of the controller*.

The question remains as to what will happen if all the axles start slipping simultaneously. In that scenario of course the present arrangement will be unable to curb the runaway slip. What can be done however is to connect the motors of the bogie to an additional motor which drives a separate load adjusted to approximately match the train's acceleration characteristics. This additional motor need not be another traction motor by any means – a small auxiliary motor with a small inverter will be sufficient so long as the ratios CK_0k_s/J and CK_0k_s/Γ for the auxiliary are more or less the same as those for the real motors. Minor mismatches in load will not be a problem as they can be countered by appropriate adjustment of φ for the auxiliary motor. The addition of a small auxiliary system will add virtually nothing to the cost and complexity of a loco bogie but will effectively check the tendency of the loco wheels to slip.

3. Additional features and concluding remarks

After (2) I had mentioned that amortisseur windings will not be required on the traction motors. This is because of the rolling without slipping condition which is ensured by the friction with the rail. The small torques typically generated by amortisseur windings will have scant chances of success in competition with the much larger forces of ground friction. Further, amortisseur windings are bulky and militate against the power density advantage which PMSM has over other types of motors. On the auxiliary motor however, amortisseur windings will be required to prevent hunting and oscillation.

One issue which has to be taken into account is the fact that different wheels of the same locomotive may have different diameter due to unequal wear and tear. The control algorithm, in the form I have described, forces all the wheels to run at the same angular velocity. This problem can be addressed in several ways. Firstly, it is known that a positive slip ratio of about 2 percent actually causes an increase in tractive effort over the non-slip case. This is the motivation behind the creep control used on certain locomotives. For the purposes of the present algorithm, if the diameter mismatch between different wheels is small then the smallest wheels can be run in non-slip mode and the larger ones in creep mode. This operation will increase the wear on the larger wheels and thus tend towards equalizing the wheel diameters. Alternatively, a delay mechanism may be incorporated in the drive so as to preferentially slow down the firing rate of the inverters connected to motors driving larger wheels. Finally, there is the option of periodically grinding all the wheels to the same diameter at the trip sheds, as is done with locomotives such as the monomotor BB 26000 mentioned in the Introduction.

I will now give a brief discussion on starting the locomotive. At low speeds, the back emf is low so it is difficult to read it correctly and control the motors. In this regime there is not much that can be done other than firing the inverter at a frequency equalling (or slightly exceeding, to anticipate the rotor's acceleration) the rotor rotation frequency, starting from a random phase. If the torque sensor registers positive, then the approach can be carried on while if it gives negative, the process must be restarted from a different initial phase. If the inverter frequency is constant, a positive start too will eventually become negative as the motor accelerates – at this point the frequency must be hiked to compensate for this effect. At the very start of motion, the approximate positions of each rotor can be determined in the same manner by applying a dc voltage from the inverter and recording the torque reading – the loco brake may be kept on in this stage so as to avoid rollback of the train. More involved, and also more accurate, starting procedures are described in [13,21]. Of course, a non-electronic starting mechanism, such as pony motors, may also be employed.

* * * * *

Acknowledgement

I am grateful to KVPY, Government of India, for a generous Fellowship.

References

[1] M Terashima, T Ashikaga, T Mizuno, K Natori, N Fujiwara and M Yada, "Novel motors and controllers for high-performance electric vehicle with four in-wheel motors," **IEEE Transactions on Industrial Electronics 44** (1), 28-38 (1997)
[2] R Dolecek, O Cerny and P Sykora, "The Traction drive of the experimental rail vehicle," **Proceedings of the 4th International Conference on Power Engineering, Energy and Electrical Drives**, 650-654 (2013)
[3] The AGV Brochure of Alstom
[4] F Blaschke, "The principle of field orientation as applied to the new closed loop transvector control systems for rotating field machines," **Siemens Review 34**, 217-220 (1972)
[5] G Pellegrino, E Armando and P Guglielmi, "Direct-flux vector control of IPM motor drives in the maximum torque per voltage speed range," **IEEE Transactions on Industrial Electronics 59 (10)**, 3780-3788 (2012)
[6] I Takahashi and T Noguchi, "A New quick response and high efficiency control strategy of an induction motor," **IEEE Transactions on Industry Applications 22** (5), 820-827 (1986)
[7] M Depenbrock, "Direct self control (DSC) of inverter-fed induction machine," **IEEE Transactions on Power Electronics 3** (4), 420-429 (1988)
[8] L Zhong and M F Rahman, "Analysis of direct torque control in permanent magnet synchronous motor drives," **IEEE Transactions on Power**

Electronics 12 (3), 528-536 (1997)
[9] G S Buja and M P Kazmierkowski, "Direct torque control of PWM inverter-fed ac motors – a survey," **IEEE Transactions on Industrial Electronics 51** (4), 744-757 (2004)
[10] M Pacas and J Weber, "Predictive direct torque control for the PM synchronous machine," **IEEE Transactions on Industrial Electronics 52** (5), 1350-1356 (2005)
[11] T M Jahns, "Flux-weakening regime operation of an interior permanent-magnet synchronous motor drive," **IEEE Transactions on Industry Applications 23** (4), 681-689 (1987)
[12] S Chaithongsuk, B N Mobarakeh, J P Caron, N Takorabet and F M Tabar, "Optimal design of permanent magnet motors to improve field-weakening performances in variable speed drives," **IEEE Transactions on Industrial Electronics 59** (6), 2484-2494 (2012)
[13] N Matsui, "Sensorless PM brushless dc motor drives," **IEEE Transactions on Industrial Electronics 43** (2), 300-308 (1996)
[14] G J Su and J W McKeever, "Low-cost sensorless control of brushless dc motors with improved speed range," **IEEE Transactions on Power Electronics 19** (2), 296-302 (2004)
[15] "Traction ferroviaire," http://sciences-physiques.ac-dijon.fr/documents/lycee/phys_app/traction_fer/traction_fer.pdf
[16] R Krishnan, "*Electric Motor Drives – Modeling, Analysis and Control*," PHI Learning Private Limited, New Delhi (2010)
[17] J L Kirtley, MIT Course no. 6.685 Electric Machines (Opencourseware), Lecture notes 9
[18] S Bhattacharjee, "Iterative solution of Maxwell's equations for an induction motor," Arxiv no. 1204.0237v2
[19] S Bhattacharjee, "*The Electromagnetism of the Induction Motor*," Lambert Academic Publishing, Saarbrucken, Germany (2013)
[20] L D Landau and E M Lifshitz, "*Classical Mechanics*," Pergammon Press, New York, USA (1976)
[21] W J Lee and S K Sul, "A New starting method of BLDC motors without position sensor," **IEEE Transactions on Industry Applications 42** (6), 1532-1538 (2006)